Link to original published version: http://dx.doi.org/10.1109/TAP.2015.2452937

Citation: AbouAlmal A, Abd-Alhameed RA, Jones SMR and Al-Ahmad H (2015) New methodology for predicting vertical atmospheric profile and propagation parameters in sub-tropical Arabian Gulf region. IEEE Transactions on Antennas and Propagation. 63(9): 4057-4068.

Author draft, IEEE Trans on Antennas and Propagation, VOL. 63, NO. 9, SEPTEMBER 2015, pp. 4057 - 4068, DOI: 10.1109/TAP.2015.2452937

New Methodology for Predicting Vertical Atmospheric Profile and Propagation Parameters in Sub-tropical Arabian Gulf Region

Abdulhadi AbouAlmal, Raed A. Abd-Alhameed, Steve MR Jones and Hussain Al-Ahmad

Abstract —**A new simplified approach is proposed to evaluate the vertical refractivity profile within the lowest 1 km of atmosphere from the analysis of surface refractivity, N_s, in areas where upper air data are not available. Upper-air measurements from the nearest available radiosonde location with similar surface profile to these sites are utilized. The profiles of N_s and refractivity extrapolated to sea level, N_o, obtained from surface meteorological data using both fixed stations and radiosonde are investigated and compared. Vertical refractivity gradient, ΔN, is evaluated at three atmospheric layer heights within the first kilometer above the ground in addition to propagation parameters relevant to each atmospheric layer. At six sites, different approaches are compared for the analysis of three important parameters; namely effective earth radius factor, k, anomalous propagation probability parameter, β_0, and point refractivity gradient at 65 m not exceeded for 1% of time, dN_1. The k-factor parameter is investigated using a new weighted average approach of ΔN at 65 m, 100 m and 1 km layers above the ground. The results are compared with the latest ITU maps and tables for the same area.**

Index Terms – **Atmospheric refraction, Refractivity gradient, effective earth radius, anomalous propagation, β_0, point refractivity gradient**.

I. Introduction

The analysis of reliable meteorological data is essential to predict fading and interference probabilities that are dominated by atmospheric refraction in the area under study. The curvature of the propagation path is determined by the value of the effective earth radius factor, which is evaluated from the prevailing meteorological conditions; such as pressure, temperature and relative humidity. The vertical refractivity profile is governed by the humidity gradients in the lowest layers of the troposphere and by the atmospheric pressure in the upper levels. However, the detailed profile is subject to random variation that is unpredictable in practice. Anomalous phenomena such as super-refraction and ducting, may occur when large negative values of refractivity gradient, ΔN, are obtained, causing the curvature of radio signals to approach the Earth curvature or to be trapped for long distances [1]. Global contour maps and statistics are provided by ITU for the surface refractivity, N_s and ΔN parameters at specified altitudes [2]. The ITU has defined a negative exponential model for the reference atmosphere and proposed a reference value of -40 N/km for the vertical ΔN over the first kilometer in temperate regions [3].

The surface meteorological data and N_s, are widely available compared with the upper air data and the point refractivity values at higher altitudes [4]. Although radiosonde is commonly used for upper air measurements, the data accuracy is affected by sensors' uncertainties that can reach up to 0.5°C, 5 % and 1 hPa for temperature, humidity and pressure parameters, respectively. Some linear and exponential models [2, 4, 5] have been proposed to estimate the vertical profile from existing N_s data. Several studies on refractivity analysis have been carried out for temperate climates all over the world [6-11], while a few are available for the unique subtropical climate of the Arabian Gulf region [12-17]. Three important atmospheric layers, namely 65 m, 100 m and 1 km layers above the ground are analyzed and the relevant propagation parameters are derived for the design of terrestrial communication systems operating in such climate.

Cumulative distributions in addition to the hourly, monthly and yearly variations are presented. The predicted results using the new models are compared with the values obtained from other relationships available in the literature. The correlation between predicted and actual available data for each parameter and the root mean square errors, RMSE, are compared.

A. Site Locations and Meteorological Data

Seventeen years of surface and radiosonde meteorological data from January 1st, 1997 to December 31st, 2013, have been gathered in the United Arab Emirates (UAE), for the analysis. The surface data are recorded hourly at six sites while upper air radiosonde data are obtained at one site from two daily ascents, nominally at 00:00 and 12:00 Universal Time (UT) which correspond to 4:00 am and 4:00 pm local time. In certain periods, only one ascent was available per day, which mostly referred to 00:00 UT. The United Arab Emirates is located in the Arabian Gulf region, which is likely to experience abnormal propagation conditions such as ducting phenomenon due to its special climate, which is hot and humid over the course of the year. More details about the radiosonde and United Arab Emirates location are introduced in [12].

Abdulhadi AbouAlmal is with Engineering Department, Emirates Telecommunication Corporation, Etisalat, UAE (e-mail: eng_abdulhadi@yahoo.com).

Abdulhadi AbouAlmal, R.A.A. Abd-Alhameed and S.M.R. Jones are with the Antenna and Applied Electromagnetics Research Group, School of Engineering Design and Technology Bradford University, Bradford, West Yorkshire, BD7 1DP, UK (e-mail: r.a.a.abd@bradford.ac.uk).

Hussain AlAhmad is with Electrical Engineering Department, Khalifa University of Science, Technology & Research (KUSTAR), Sharjah, UAE.

Abu Dhabi (AUH), Dubai (DXB), Sharjah (SHJ), and Ras Al-Khaimah (RAK) are four coastal sites located nearby the Arabian Gulf where the climate is usually hot and humid over the course of the year. Al-Ain (AIN) is an inland city with lower humidity. Al-Fujairah (FUJ) is coastal city nearby Oman Gulf that is also hot and humid but nearby the tropical zone where the gulf opens to the Indian Ocean. This location of Al-Fujairah results in a special climate in comparison with the other Emirates [14]. The geographical locations of the six sites are shown in United Arab Emirates map in Fig. 1.

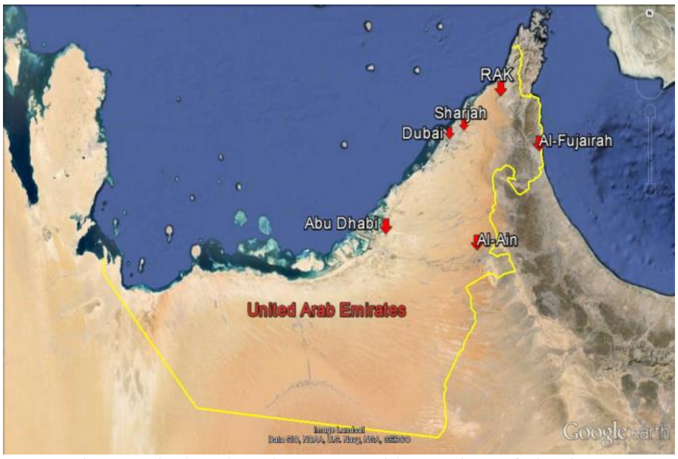

Fig. 1. United Arab Emirates Map with Locations of Six Sites

The site coordinates and altitudes above the sea level are provided in Table 1. All the sites have similar height around 30 m above sea level, except Al-Ain (AIN), which is located in a mountainous area.

TABLE 1: LOCATIONS OF SURFACE METEOROLOGICAL STATIONS

Site	Latitude [ºN]	Longitude [ºE]	Altitude (m)
AUH	24.43	54.64	27
DXB	25.25	55.36	36
SHJ	25.32	55.52	33
RAK	25.62	55.94	34
AIN	24.26	55.62	262
FUJ	25.11	56.33	21

Radiosonde data are available for 9462 radiosonde ascents. Due to low quality or incomplete ascents, data for June 1998, April 2000, November 2005, June 2006 to November 2006 and January 2010 to May 2010 are not available. From December 2006 to December 2008, the data of only one ascent, mostly at 00:00 UT, is available on daily basis. In addition, a small number of abnormal values have been excluded owing to faulty readings from the instrument.

B. Models of Refractivity

The refractivity, N, in N-units consists of dry and wet components and can be evaluated at either the ground or higher altitudes using the well know expression [2, 5]. The dry component contributes to around 60 to 80 % of the overall value [9]. In the standard atmosphere, N decreases with altitude since the total pressure drops off rapidly while temperature decreases with height [18]. In areas where radiosonde upper-air data are not available, several relationships can be used to predict upper refractivity, N_h, at a certain altitude, h, from the surface refractivity, N_s, obtained from the commonly available surface meteorological measurements [4, 5]. ITU exponential models can be used to calculate N_h and refractivity values extrapolated to sea level, N_o, from the available surface data including N_s, the surface altitude from sea level, h_s, and the height coefficient with respect to the sea level, h_o, in km [2, 5]

$$N_h = N_s \, . \, e^{\left[-\left(\frac{h-h_s}{h_o}\right)\right]} \qquad (\mathrm{N-units}) \qquad (1)$$

The vertical refractivity gradient, ΔN, in N-units per km (N/km) usually has a negative value causing the rays to bend towards the ground. In the linear model, ΔN can be obtained from two refractivity values, N_s at the surface, h_s, and N_h at an altitude h, by dividing the refractivity difference (N_s - N_h) over (h_s - h) [5, 19]. A close correlation is observed between N_s and N_h within the first 100 m of atmosphere and between N_s and ΔN at 1 km layer above ground [17]. ΔN can be estimated from N_s using the following exponential decaying relationship for the first kilometer, ΔN [17]:

$$\Delta N = a \, . \, (1 - e^{-b \, . \, N_s})^c \qquad (\mathrm{N/km}) \qquad (2)$$

where the values of coefficients a, b, and c are found to be -316.54734, 0.00958 and 37.85049, respectively. It is noted that these coefficients may vary from one place to another and for different study periods within the same location. Long-term data are required to provide accurate estimations. Other models are studied to also predict the vertical ΔN near the ground from the measurements of electromagnetic wave strength and diffraction losses [20, 21]. In order to extend these relations to other regions around the world, the correlation between the estimated data and the measured values needs to be evaluated.

C. Important Propagation Parameters

For microwave link design, some parameters must be set carefully as input data to optimize the link performance. Two of these parameters are particularly important, the effective earth radius factor, k, which is commonly set as a standard value of 4/3, and point refractivity gradient not exceeded for 1% of time, $dN_{1\%}$, at 65 m layer of atmosphere [22]. Estimated values of $dN_{1\%}$ and anomalous propagation probability parameter, β_0, are provided by ITU tables for different geographical locations whenever reliable local data are not available [2].

Effective earth radius factor, *k*: The effective earth radius is the radius of a hypothetical spherical Earth, without atmosphere, for which propagation paths follow straight lines while the heights and ground distances being the same for actual Earth with atmosphere and constant vertical gradient of refractivity [1, 13]. The k-factor can be calculated from the rate of change of the refractive index with height and the actual Earth's radius, a, using Snell's law in spherical geometry, knowing that $N = (n\text{-}1) \times 10^6$, where a is given by unit of nmi (a = 6371 km = 3440 nmi). The k-factor value must be multiplied by the actual Earth's radius, a, in order to plot the propagation paths as straight lines [1, 3]. The k-factor can be derived from the vertical refractivity gradient in the first kilometer above the ground, ΔN_1, assuming that gradient of refractive index is constant with height, at least over the lower atmospheric layer up to 1 km [1, 22]. ITU suggests global standard values of ΔN_1 for reference atmosphere and corresponding k-factor, which are -40 N/km and 4/3, respectively [3]. As an alternative, a new weighted average approach of ΔN values at the three atmospheric layers of 1 km and below is used in this work to accurately evaluate k-factor considering the vertical variations of refractive index near the ground below 100 m, where most terrestrial wireless systems operate. The refractive conditions are related to the values of k-factor. For example, if the ITU reference k-factor value of 4/3 is considered, which refers to a normal refraction condition in a standard atmosphere, the positive k-factor values below 4/3 indicates the incidence of sub-refraction, where signals bend upward. The occurrence of super-refraction is indicated by positive k-factor values larger than 4/3. Negative values of k-factor refer to the incidence of ducting phenomenon, where the wireless signal gets trapped within two layers and travels for long distances over the horizon.

Anomalous propagation probability parameter, β_0: The vertical refractivity gradient, in the lowest 100 meters of the troposphere above the ground surface, is an important parameter to estimate propagation effects such as ducting, surface reflection and multipath on terrestrial line-of-sight links. The β_0 parameter represents occurrence probability of non-standard propagation and its statistics are derived from the cumulative distributions of the vertical ΔN at the first 100 m layer. β_0 is obtained from the percentage of time in which ΔN value is less than or equal to -100 N/km.

Point refractivity gradient "$dN_{1\%}$": is the point ΔN value at the lowest 65 m of the atmosphere not exceeded for 1% of an average year [22, 23], which is used for predicting microwave links' availability.

D. *New Methodology for Vertical ΔN Prediction*

New approaches are used to simplify and improve the accuracy of vertical ΔN evaluation in areas where upper air data are not available. In approach 1, only measured refractivity parameters at surface and higher altitudes are utilized to estimate ΔN. The surface refractivity profiles for a number of sites are compared. For sites with similar surface conditions to a site in the surrounding region with available radiosonde measurements, upper-air refractivity obtained from radiosonde can be utilized to estimate the vertical profile in the surrounding sites, where only surface data are available. This is based on the assumptions that most of the land and sea interactions occur at ground level, while atmosphere gets more horizontally homogenous at higher altitudes and the vertical N_h is assumed to be more stable. Although poor correlation has been observed between N_s and ΔN at 65 m and 100 m layers compared with good correlation at 1 km [17], this new approach aims at improving the accuracy of estimated N_h values at these altitudes by using real radiosonde measurements in case of similar surface profiles. Consequently, the results of ΔN at these layers are expected to be improved as well, when the linear ΔN model is used. The sites can be selected such that they are located within few hundred miles from a radiosonde location that have similar surface weather conditions. In this approach, vertical profile at all sites are evaluated as follow:

a) The measured surface and upper-air data are obtained from radiosonde, which is available at the AUH site only. The measured ΔN at a particular altitude, h, is calculated using the linear model.
b) N_s is calculated from surface data measured using fixed surface stations at AUH and surrounding sites. The N_h parameter is obtained from radiosonde measurements available at the AUH site only. At 65 m and 100 m, the measured N_h at AUH is utilized at the surrounding sites with similar surface refractivity profiles to AUH. At 1 km layer, N_h is applied for all six sites since the atmosphere get much more homogeneous at this high altitude. ΔN is then calculated from measured N_s and N_h using the linear model. Note that for the AUH site only, measured ΔN obtained using methods (a) and (b) are compared, in order to evaluate the radiosonde data accuracy.

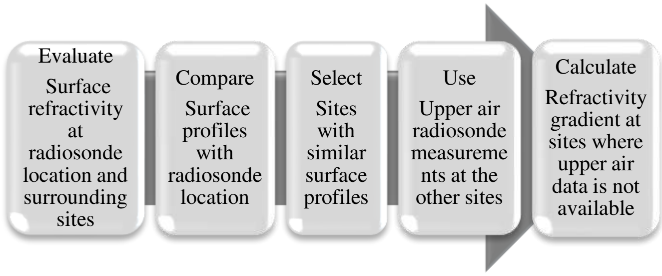

Fig. 2. Flow diagram of Approach 1-(b)

In the second approach 2, ΔN is obtained from measured N_s at the surface and predicted N_h at higher altitudes using empirical relationships, which are derived from radiosonde measurements at a single site. These models are used to predict the vertical refractivity profiles at the surrounding sites where only surface data are available. In this approach, ΔN is estimated from measured N_s and predicted N_h subject to the correlation observed between N_s and either N_h or ΔN at different altitudes [17] as follows:

a) N_h is predicted using exponential model, e.g. equation (1), from measured N_s. Predicted ΔN is then calculated using the linear model. At 65 m and 100 m layers, it has been observed that N_s is correlated with N_h.
b) Predicted ΔN is directly estimated from measured N_s using exponential model (2). At 1 km layer, N_s is found to be correlated with ΔN.

The relationships between N_s and either N_h or ΔN for predicting the vertical refractivity profiles are investigated in comparison with the new approaches introduced in this study. The results of the new approaches and predicted N_h and Δ*N* are compared at certain sites to confirm the earlier correlation findings at different layers. To the best of our knowledge, the proposed approach to estimate the vertical refractivity profile based on analysis of the similarities in surface profiles, in addition to the use of weighted average approach to evaluate the *k*-factor from mean and median of Δ*N* at different atmospheric layers, has not been investigated before.

II. Analysis and Results

Δ*N* statistics for the first three atmospheric layers above the ground, 65 m, 100 m and 1 km, where terrestrial communication systems operate, are important to be investigated due to their contributions to several propagation studies. For example; the first two layers, 65 m and 100 m, are essential for estimating the point refractivity gradient not exceeded for 1% of time, which is required for availability calculations for terrestrial microwave links [23], and the occurrence probability of ducting and multipath conditions [2, 22]. It is noticed that the extreme atmospheric stratification tends to occur in layers less than 100 m thickness, which can be extended horizontally over long distance at certain times. The 1 km layer analysis is important for the estimation of the effective Earth radius factor [22, 23]. These parameters have to be carefully considered when studying the performance of terrestrial line of sight communication systems.

A. Surface Refractivity Analysis

The analysis of surface refractivity, N_s, and its dry and wet components, N_{s_D} and N_{s_W}, in addition to the N_o analysis are based on the surface SYNOPS meteorological data measured by the available fixed surface weather stations at all sites. The mean monthly distributions of N_s over the whole period is shown in Fig. 3 for the six sites. The dry refractivity component, N_{s_D}, at all sites follows the same monthly variation curve with similar values fluctuating from 250 to 272 with a span of 22 units. The monthly variation curves of N_s are dominated by the wet component, N_{s_W}, which is compensated by the inversely varying dry refractivity term, N_{s_D}. Fig. 3 shows that N_s profiles in four sites; namely AUH, DXB, SHJ and RAK, are similar with peak values shown in summer season. The monthly means of N_s vary within a range of around 82 units at all sites where a maximum monthly difference of 62 units between the six sites is observed in August. The highest monthly values and variation of N_s are observed at FUJ site with a span of 61.6 units, from 333.5 up to 395.1 N-units. This can be attributed to its location as a coastal city nearby Oman Gulf within a mountainous area, with a humid climate. AIN site has lower N_s values and monthly variations than the other sites with a span of 21 units, from 313.2 up to 334.5 N-units. This trend is due to its location as an inland city at a distance of about 100 km away from the sea with dry and low humidity weather. Similar initial results were reported for the area under study [14].

For easy reference, the ITU provides global maps of the median value (50%) of N_{s_W} exceeded for the average year [2]. Table 2 provides the values of calculated N_{s_W} at the six sites in comparison with the ITU map for United Arab Emirates. In general, it has been observed that ITU values underestimate N_{s_W} in the area under study, where the long-term median calculated values exceed 60 N-units for all sites.

The mean monthly N_o variations in the six sites are also compared with ITU maps [2] in Table 3. The ITU maps are derived using h_o = 9.5 km for the months of February and August. N_o has been calculated using two values, 9.5 km and 7.35 km, of h_o parameter. For reference purpose, the ITU has also proposed an average global profile based on N_o and h_o values of 315 N-units and 7.35 km [2]. It has been noted that h_o value varies slightly across particular atmospheric layers which have marginal impact on the refractivity predictions. The results for the winter season, February, are more consistent with the ITU values than the summer, August, except at certain sites such as AIN in case of February and FUJ in case of August. In August, the results at AUH, DXB, SHJ, and RAK are up to 14.2% less than ITU. AIN shows exceptional differences of 24.8 units and 55.4 units less than the ITU values for February and August, respectively. This can be attributed to the inland location with dry climate of the AIN site.

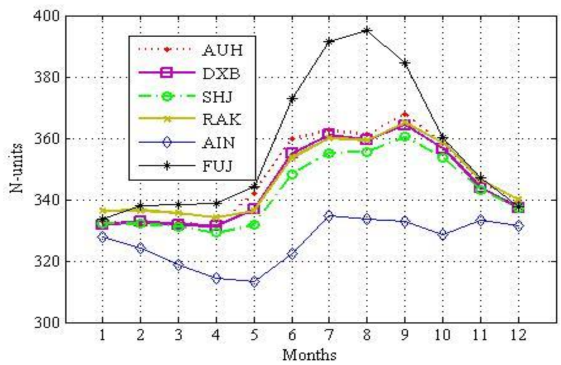

Fig. 3. Mean monthly variations of surface refractivity, N_s (1997-2013)

TABLE 2: COMPARISON OF CALCULATED N_{s_W} EXCEEDED FOR 50% OF THE YEAR WITH ITU MAP [2]

	N_{s_W} [N-units]
ITU values	60-75
AUH	81.2
DXB	81.7
SHJ	78.3
RAK	82.5
AIN	63.1
FUJ	93

TABLE 3: COMPARISON OF CALCULATED N_o WITH ITU MAPS [2]

	Coefficient h_o	February N_o	August N_o
ITU Maps	9.5	350	390
AUH	9.5	332.6	362.1
	7.35	332.9	362.4
DXB	9.5	333.8	360.3

	7.35	334.1	360.6
SHJ	9.5	333.1	356.5
	7.35	333.3	356.8
RAK	9.5	337.4	360.3
	7.35	337.7	360.6
AIN	9.5	325.2	334. 6
	7.35	325.5	334.9
FUJ	9.5	338.8	396.2
	7.35	339.1	396.6

Fig. 4 shows the average yearly variations of N_s at all sites over the whole period from 1997 to 2013. The yearly curves for AUH, DXB, SHJ and RAK follow a similar trend and the annual means are bounded within 12 units for most years. The year to year variation at these four sites is generally smooth with some peak values in 1998 at AUH and 2003 at FUJ. AIN has the lowest values and the most significant variation within a range of around 23 units, from 313 up to 336 N-units. The highest N_s values are generally shown at FUJ, except in 1998.

The cumulative distributions of N_s at the six sites are given in Fig. 5 over the whole period. The values vary from around 252 up to 601 N-units with a span of 349 units. N_s oscillates in an interval of 52 units from one site to another. Almost the lowest and highest values for all time percentages are shown at AIN and FUJ, respectively, apart from some exceptional cases such as at AUH where values exceed 460 units for around 0.5% of the total time. This exceptional value at AUH can be attributed to the peak values observed in 1998.

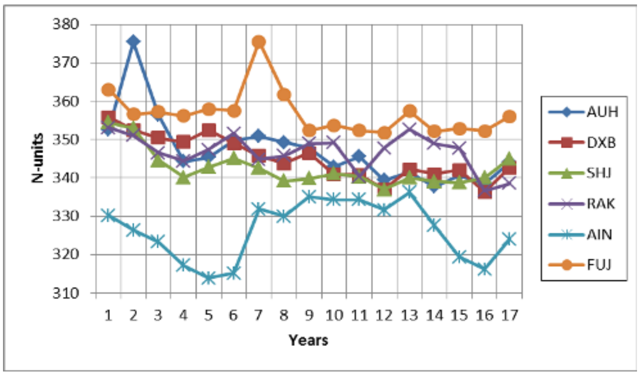

Fig. 4. Mean yearly variations of surface refractivity, N_s (1997-2013)

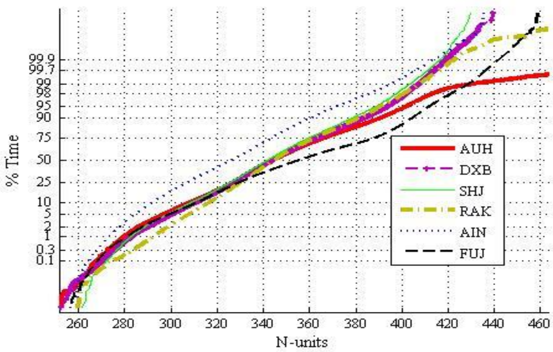

Fig. 5. Cumulative distributions of surface refractivity, N_s (1997-2013)

The results obtained from the monthly, yearly and cumulative distributions show that the surface refractivity profile at four sites; namely AUH, DXB, SHJ and RAK, are similar. Accordingly, the vertical refractivity profiles at these sites are expected to be more consistent since the atmosphere is assumed to get more horizontally homogenous with height.

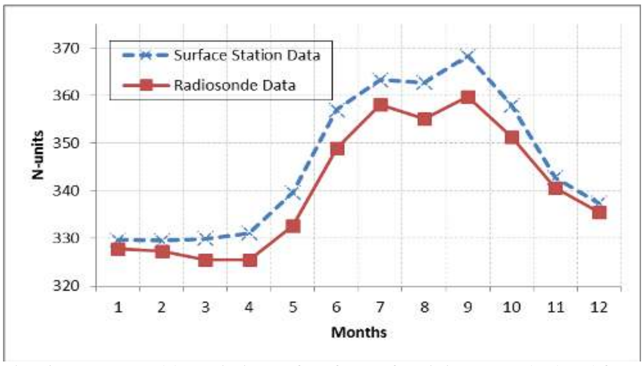

Fig. 6. Mean monthly variations of surface refractivity, N_s, calculated from fixed surface weather station and Radiosonde (1997-2013)

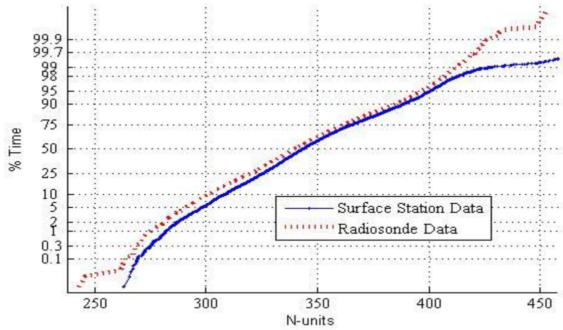

Fig. 7. Cumulative distributions of surface refractivity calculated from fixed surface weather station and Radiosonde (1997-2013)

B. Comparison of Surface Measurements

The surface meteorological data can be measured using either surface weather stations or radiosonde at the ground. The radiosonde measurements at AUH site have been compared with the surface meteorological measurements using AUH surface weather station at only two times daily due to the radiosonde data availability. This is an indication for the radiosonde data accuracy compared with the stable fixed weather sensors at the ground. The monthly and cumulative distributions of measured N_s using both data types are shown in Fig. 6 and 7. Fig. 6 shows that the monthly means of N_s measured from the surface station are larger than the values obtained from the radiosonde at all months, with a maximum difference of 8.5 units within a span of 2.5%. The N_s values measured by the radiosonde are also found to be lower for all time percentages as shown in Fig. 7. It has been found that the N_s value oscillates between 329.5 and 368.3 N-units for the surface station with a span of 38.8 units, whereas they vary from 325.5 to 359.8 N-units for the radiosonde.

The cumulative distributions of four surface meteorological parameters; namely atmospheric pressure, dry air temperature, relative humidity and water vapour pressure, measured by fixed surface station and radiosonde are analyzed at AUH site. The parameters measured by surface station has higher values for most time percentages, except for dry air temperature where radiosonde measurements are higher. This is the reason for obtaining higher N_s values for surface station at all-time percentages since the refractivity is directly proportional with pressure and vapour pressure while it is inversely proportional to the dry temperature.

C. Refractivity Gradient Analysis

The ΔN parameter has been evaluated using different approaches. For the sites with similar surface refractivity profile to AUH, the same radiosonde data are utilized for upper layers. The measurement accuracy of surface weather stations is assumed to be higher than the radiosonde at the ground level. Consequently, the reference ΔN profile at the AUH site is calculated using approach 1-(b) from both the surface measurements at the ground and radiosonde measurements at higher altitudes. Figs. 8 to 10 provide comparisons of mean monthly variations of ΔN at 65 m ($\Delta N_{0.065}$), 100 m ($\Delta N_{0.1}$) and 1 km (ΔN_1) layers, using different approaches at the AUH site. The curves of ΔN_1 obtained from 1-(a) and 1-(b) approaches are more consistent with a maximum monthly difference of 8 units. The differences between ΔN values obtained using 1-(a) and 1-(b) approaches increase considerably up to 74 and 55 units at the 65 m and 100 m layers, respectively. The higher differences at the low altitudes can be attributed to the fact that any small change in N_s value results in large disagreement in ΔN due to the low decimal number in the denominator of the linear ΔN equation.

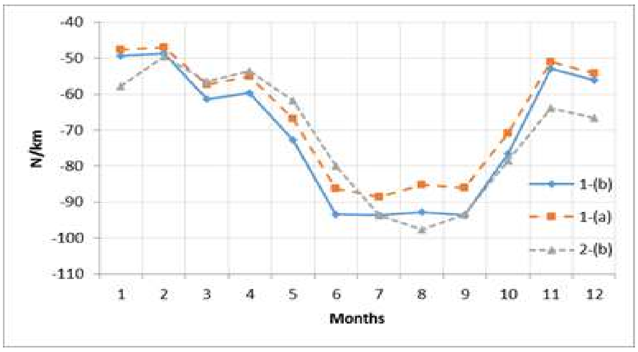

Fig. 8. Comparison of mean monthly variations of ΔN at 1 km at AUH

The root mean square error, RMSE, and correlation coefficients are evaluated at AUH site between the measured or predicted ΔN values using approaches 1-(a), 2-(a) and 2-(b) with reference to the measured ΔN using 1-(b) approach. Table 4 summarizes the obtained results. The correlation between ΔN and N_s at low altitudes, 65 m and 100 m, is found to be poor while good correlation is observed at 1 km height. Similar results have been reported [17]. At 1 km height, 2-(b) approach gives the highest correlation coefficient and minimum RMSE value noting that good correlation has been observed between ΔN and N_s, while 2-(a) gives the highest RMSE result. At 65 m and 100 m layers, 2-(a) approach shows marginal improvement compared to 2-(b), although poor correlation has been found between ΔN and N_s at these low altitudes [17].

Fig. 11 shows the scatter diagram for the ΔN_1 values obtained using 1-(b) and 2-(b) approaches. The coefficient of

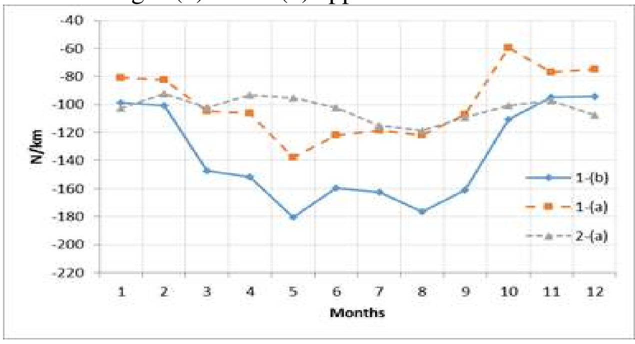

Fig. 9. Comparison of mean monthly variations of ΔN at 100 m at AUH

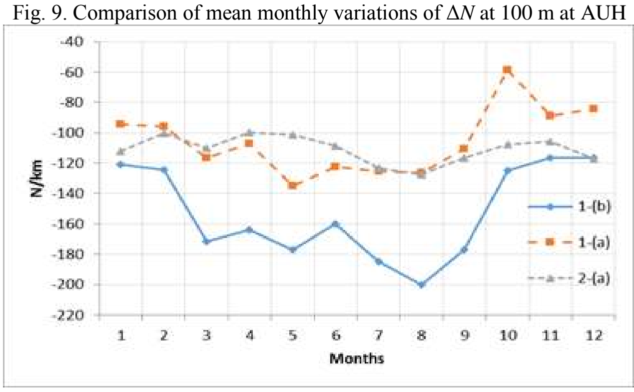

Fig. 10. Comparison of mean monthly variations of ΔN at 65 m at AUH

TABLE 4: CORRELATION AND RMSE VALUES OF ΔN RESULTS WITH REFERENCE TO RADIOSONDE DATA

Layer	Approach / Model	Correlation	RMSE
1 km	1-(a)	0.857	20.4
	2-(a)	0.859	35.2
	2-(b)	0.86	18.8
100 m	1-(a)	0.49	200.7
	2-(a)	0.41	216.8
	2-(b)	0.4	219.8
65 m	1-(a)	0.38	322.8
	2-(a)	0.4	337.9
	2-(b)	0.39	337.9

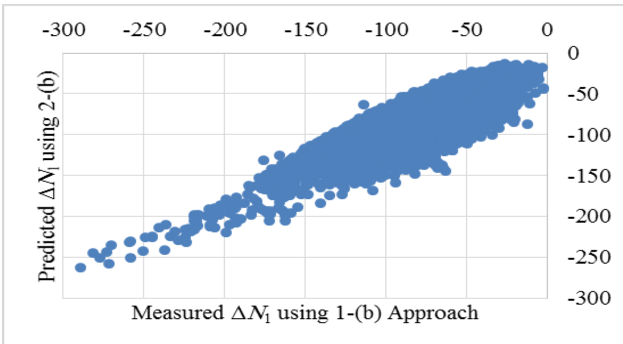

Fig. 11. Scatter diagram for ΔN at 1 km at AUH, obtained using 1-(b) and 2-(b) approaches

determination is found to be 0.86, which means that significant correlation exists with minimum error. Fig. 12

shows the mean monthly variations of ΔN_1 calculated using the 1-(b) approach for all six sites. The monthly ΔN values oscillate approximately between 125.5 and -48.8 N/km with a span of 76 units. Fig. 13 shows the mean monthly distributions of ΔN_1 obtained using 2-(b). The ΔN_1 values range from -134 to -36.7 N/km with a span of 97.3 units. The curves of ΔN_1 are found to be similar to N_s at AUH, DXB, SHJ and RAK sites, where refractivity profiles are almost consistent with peak values shown in the summer. The ranges of monthly variations at these four sites are found to be around 49 units, from -97.7 to -48.8 N/km, and 51.9 units, from -101.5 to -49.6, for approaches 1-(b) and 2-(b), respectively. The highest monthly variations of ΔN_1 has also been observed in the FUJ site within a span of 73.4 units, from -125.5 to -52 N/km, and an interval of 78.5 unites, from -134 to -55.4 N/km, using approaches 1-(b) and 2-(b), respectively. This can also be attributed to its special location and climate.

The lowest absolute ΔN_1 values are given during winter time with some exceptional cases such as May for AIN site in Fig. 13 when the 2-(b) approach is used. On the other hand, the summer season shows the highest absolute ΔN_1 values at all sites, in particular for the months of June, July, August and September.

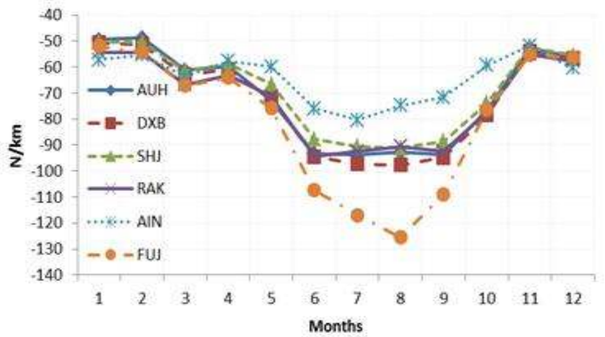

Fig. 12. Comparison of mean monthly variations of ΔN_1 at all sites using 1-(b) (1997-2013)

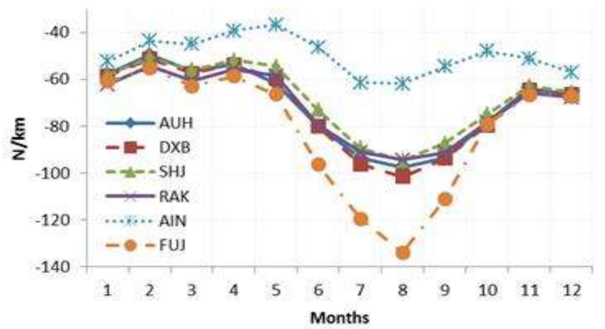

Fig. 13. Comparison of mean monthly variations of ΔN_1 at all sites using 2-(b) (1997-2013)

In Table 5, the absolute values of mean monthly ΔN_1 are compared with the corresponding values in the ITU maps [2] for the months of February, May, August and November. For the AUH, DXB, SHJ and RAK sites, the ΔN_1 results of May and August are more consistent with ITU values than February and November, when the 1-(b) approach is used. The differences with ITU values are found to be up to 21.2 and 17.6 units, for February and November, respectively. Similar results have been reported before [14]. Higher inconsistencies have been observed for May and August using the 2-(b) approach, where the differences are found to be up to 25.5 and 11.5 units, respectively. All proposed ITU values for ΔN_1 are overestimated in comparison with the results obtained in this study.

TABLE 5: COMPARISON OF ABSOLUTE MONTHLY ΔN_1 RESULTS USING 1-(b) AND 2-(b) APPROACHES WITH ITU

	February		May		August		November	
Approach	1-(b)	2-(b)	1-(b)	2-(b)	1-(b)	2-(b)	1-(b)	2-(b)
ITU	70		80		90		70	
AUH	49	50	73	62	93	98	53	64
DXB	51	51	72	60	98	102	54	65
SHJ	51	51	67	55	91	95	52	63
RAK	54	54	71	59	91	94	55	66
AIN	55	44	60	37	75	62	52	51
FUJ	54	55	76	66	126	134	55	67

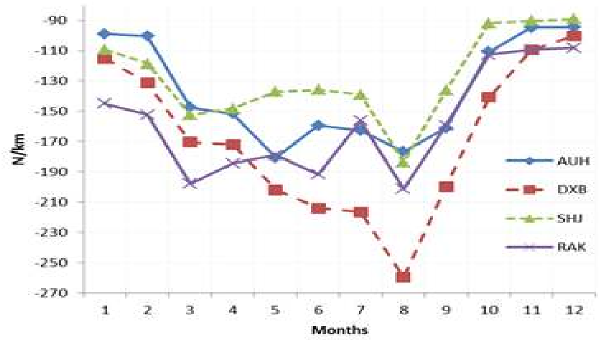

Fig. 14. Comparison of mean monthly variations of $\Delta N_{0.1}$ at all sites using 1-(b) approach (1997-2013)

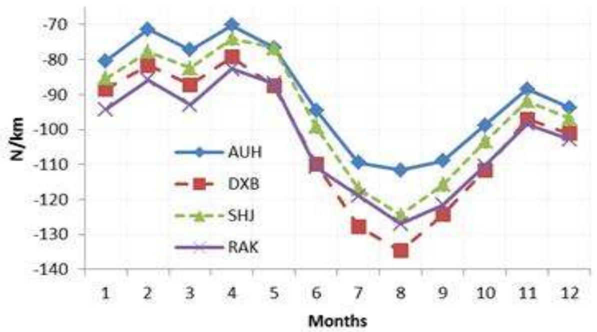

Fig. 15. Comparison of mean monthly variations of ΔN0.1 at all sites using 2-(a) approach (1997-2013)

Figs. 14 and 15 show the mean monthly variations of ΔN at 100 m, $\Delta N_{0.1}$, using approaches 1-(b) and 2-(a), respectively, at the AUH, DXB, SHJ and RAK sites. Using 2-(a) at the four sites, low $\Delta N_{0.1}$ values are observed during winter and the highest absolute values are shown in summer season. Similarly, the mean monthly distributions of $\Delta N_{0.065}$ at 65 m have similar seasonal variations using the 2-(a) approach. When the 1-(b) approach is used, the monthly distributions of ΔN at 100 m and 65 m layers are not coherent at the four sites. However, the AUH and DXB sites have similar seasonal variations at all atmospheric layers when both approaches are used. Using the 1-(b) approach, the ranges of $\Delta N_{0.1}$ and $\Delta N_{0.065}$ vary from -259.5 to -89 N/k and from -295 to -107.6 N/km, respectively. The maximum monthly differences between the four sites at 100 m and 65 m layers are found to be 83 and 103 units, respectively. This gives a clear indication that the prediction of Δ*N* is much more complicated at lower altitudes.

D. Analysis of k-factor Profile

The mean monthly ΔN_1 values at the AUH site vary between -97.62 and -47.1 N/km and the corresponding *k*-factor ranges between 1.43 to 2.64 when all three approaches, 1-(a), 1-(b) and 2-(b) are applied, as shown in Fig. 16. The *k*-factor distributions at AUH using all approaches are found to always exceed the proposed ITU standard atmosphere value of 4/3.

Fig. 17 provides the mean monthly variation of *k*-factor at the six sites using the 1-(b) approach. The monthly values of *k*-factor at all sites oscillate from 1.45 to 2.65, with some exceptional results up to 4.98 in August for the FUJ site Using the 2-(b) approach, the *k*-factor is found to vary from 1.46 to 2.83 with some exceptional values up to 6.81 at August for FUJ as well.

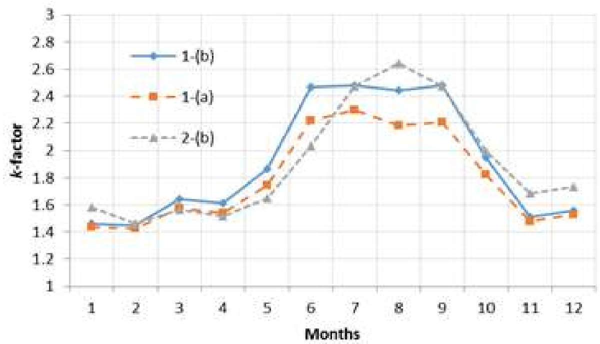

Fig. 16. Comparison of monthly variations of *k*-factor at AUH based on 1-(a), 1-(b) and 2-(b) approaches (1997-2013)

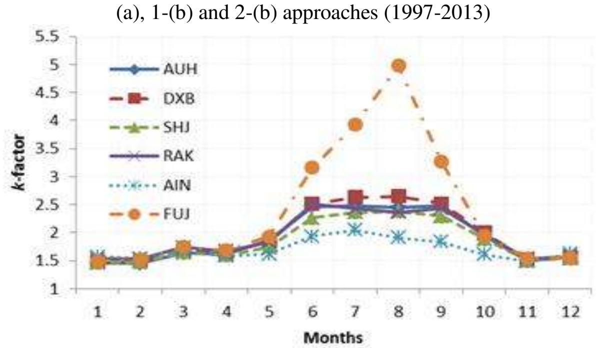

Fig. 17. Comparison of monthly variations of *k*-factor at six sites based on 1-(b) approach (1997-2013)

Table 6 summarizes the *k*-factor values obtained from the long-term mean and median results of ΔN_1 using three approaches, 1-(a), 1-(b) and 2-(b) at the six sites over the whole period from 1997-2013. At AUH, the long-term median values of ΔN_1 and *k*-factor using the 1-(b) approach are found to be -75.14 N/km and 1.92, respectively. The highest *k*-factor value of 2.4 is obtained at FUJ site based on ΔN_1 results. It has been noted that median *k*-factor is less than mean value by approximately 0.2.

The *k*-factor has also been calculated from the mean Δ*N* values at 65 m and 100 m layers, where most of terrestrial wireless systems operate. A weighted average approach for evaluating mean and median Δ*N* among the three layers has been used for obtaining more appropriate *k*-factor value to be applied for the path clearance analysis of microwave links operating within the first 150 m layer above the ground. Antennas on these microwave systems are found to be fixed at around 55 m to 150 m height above the sea level. For simplicity, similar weights have been assigned to the mean and median Δ*N* values at 65 m, 100 m and 1 km. As given in Table 6, the value of *k*-factor calculated from the long-term mean weighted average Δ*N* using the 1-(b) approach at the DXB site is found to be negative, which indicates the prevalence of ducting in the area under study.

TABLE 6: COMPARISON OF ΔN_1 AND *k*-FACTOR RESULTS WITH ITU VALUES FOR REFERENCE ATMOSPHERE

	Approach	Median	Mean	Median k-factor	Mean k-factor
ITU	-	-40		1.33	
From ΔN1					
AUH	1-(a)	-71.11	-74.48	1.83	1.90
	1-(b)	-75.14	-79.60	1.92	2.03
	2-(b)	-74.88	-79.76	1.91	2.03
DXB	1-(b)	-78.15	-81.48	1.99	2.08
	2-(b)	-76.97	-80.67	1.96	2.06
SHJ	1-(b)	-74.14	-77.40	1.89	1.97
	2-(b)	-73.60	-76.63	1.88	1.95
RAK	1-(b)	-76.65	-79.85	1.95	2.04
	2-(b)	-75.39	-78.90	1.92	2.01
AIN	1-(b)	-64.96	-71.83	1.71	1.84
	2-(b)	-51.51	-55.85	1.49	1.55
From Weighted Average of ΔN1, ΔN0.1 and ΔN0.065					
AUH	1-(a)	-81.35	-98.58	2.08	2.69
	1-(b)	-112.41	-143.8	3.52	11.85
	2-(b)	-74.12	-78.97	1.89	2.01
DXB	1-(b)	-144.25	-170.4	12.32	-11.69
	2-(b)	-76.13	-79.84	1.94	2.03
SHJ	1-(b)	-117.80	-128.4	4.01	5.49
	2-(b)	-72.81	-75.85	1.86	1.93
RAK	1-(b)	-145.49	-152.8	13.64	37.45
	2-(b)	-74.59	-78.07	1.91	1.99
FUJ	1-(b)	-81.35	-98.58	2.08	2.69
	2-(b)	-112.41	-143.8	3.52	11.85

E. $\Delta N_{0.1}$ at 100 m Layer and β_0 Analysis

The cumulative distributions of $\Delta N_{0.1}$ at the AUH site for different times using the 1-(a), 1-(b) and 2-(a) approaches are shown in Fig. 18. $\Delta N_{0.1}$ values for all time percentages approximately oscillate between -1641 and 590 N/km for the 1-(b) approach, and between -1207 and 580 N/km for the 1-(a) approach, with some exceptional values outside these ranges. The long-term β_0 values at AUH are found to be 45.3%, 57.3% and 56.5% using approaches 1-(a), 1-(b) and 2-(a), respectively. Considering the reference results for the

Author draft, IEEE Trans on Antennas and Propagation, VOL. 63, NO. 9, SEPTEMBER 2015, pp. 4057 - 4068, DOI: 10.1109/TAP.2015.2452937

1-(b) approach, the value of $\Delta N_{0.1}$ is expected to be less than or equal to -100 N/km for around 57.3% of the time.

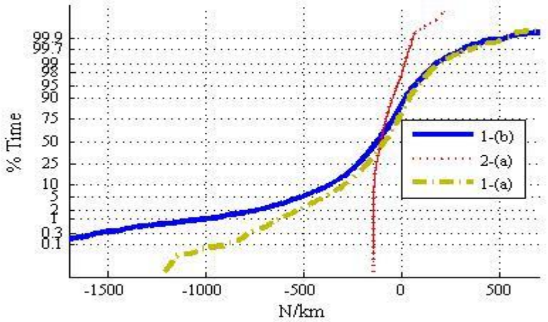

Fig. 18. Comparison of cumulative distributions of $\Delta N_{0.1}$ at AUH using 1-(a), 1-(b) and 2-(a) approaches (1997-2013)

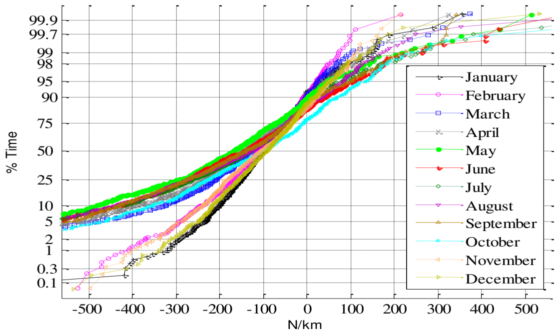

Fig. 19. Monthly cumulative distributions of $\Delta N_{0.1}$ at AUH using 1-(b) approach (1997-2013)

TABLE 7: MONTHLY β_0 VALUES (%) USING DIFFERENT APPROACHES AT AUH COMPARED WITH ITU MAPS

Months	ITU Values	1-(a)	1-(b)
February	30	46.7	55.9
May	75	58	69.1
August	70	43.8	57.5
November	40	42.7	52.1

Fig. 19 shows the monthly cumulative distributions of $\Delta N_{0.1}$ at AUH using the 1-(b) approach. For 50% of the time, the summer season shows higher $\Delta N_{0.1}$ than winter with peak values obtained in May. The monthly β_0 variations obtained from $\Delta N_{0.1}$ distributions using approaches 1-(a) and 1-(b), are compared with ITU maps in Table 7. It has been noted that ITU values are not in good agreement with the results obtained in this study. With reference to the results of the 1-(b) approach, the estimated ITU values are below those calculated in the case of February and November with differences of around 46% and 23%, respectively, which are larger than the differences reported for the same months in an earlier study [24], which are 34% and 21%, respectively. Also, the ITU values are found to be overestimated for the months of May and August, with differences of 8.5% and 21.7%, compared with 7% and 19% reported for the same months before [24]. These differences have also been observed in other countries [9] and can be attributed to the fact that ITU maps [2] were interpolated from radiosonde data from only 99 sites worldwide between 1955 and 1959. In addition, ITU maps are usually derived from measurements performed largely in temperate regions of the world such as Europe, North America and Japan [25], which have different climatic conditions from the Gulf region.

The cumulative distributions of $\Delta N_{0.1}$ using the 1-(b) approach at the four sites with similar surface refractivity profiles are provided in Fig. 20. The long-term β_0 values obtained using approach 1-(b) are found to be 57.3%, 62.1%, 56.5% and 60.9% at AUH, DXB, SHJ and RAK, respectively. The monthly β_0 variations at these sites are compared in Fig. 21. The monthly β_0 values oscillate between 44.3% and 71.1%. Generally, summer months show higher probability of anomalous propagation at all sites. RAK has the highest β_0 values for the first four months from January to April, while DXB site shows the highest probabilities of anomalous conditions for the remaining months from May to December. Table 8 summarizes the monthly β_0 values obtained from the distributions of $\Delta N_{0.1}$ at the four sites using the 1-(b) approach.

The monthly β_0 results at the four sites are compared with ITU maps [22] in Table 9. Generally, the ITU values are under-estimated for the months of February and November at the four sites, while they are overestimated for May and August.

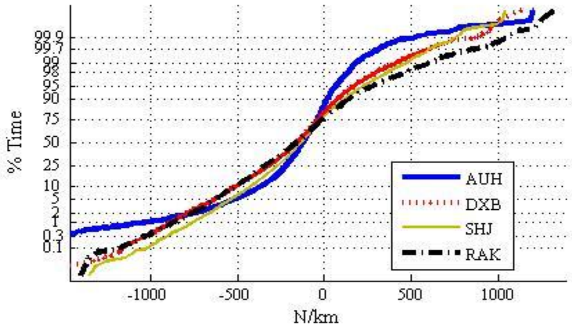

Fig. 20. Comparison of cumulative distributions of $\Delta N_{0.1}$ at 4 sites using 1-(b) approach (1997-2013)

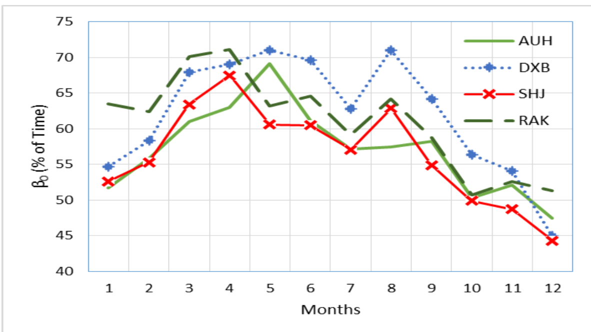

Fig. 21. Monthly variations of β0

The cumulative distributions of $\Delta N_{0.065}$ are obtained using the 1-(a), 1-(b) and 2-(a) approaches at AUH. $\Delta N_{0.065}$ values for all time percentages approximately oscillates between -2750 and 1400 N/km for the 1-(b) approach, and between -1860 and 1543 N/km for the 1-(a) approach, with some exceptional values outside these ranges. The long-term value of $dN_{1\%}$ at AUH is found to be -722.5, -1604.5 and -228.2 N/km, using approaches 1-(a), 1-(b) and 2-(a), respectively.

TABLE 8: MONTHLY β_0 VALUES (%) AT 4 SITES BASED ON 1-(b) APPROACH (1997-2013)

Months	AUH	DXB	SHJ	RAK
Jan	51.7	54.7	52.6	63.5
Feb	55.9	58.3	55.3	62.4
Mar	61	68	63.4	70.1
Apr	63	69	67.5	71.1
May	69.1	71	60.6	63.2
Jun	61.1	69.6	60.5	64.6
Jul	57.2	62.8	57.1	59.1
Aug	57.5	71	62.9	64.2
Sep	58.2	64.2	54.9	58.7
Oct	50.3	56.4	49.9	50.7
Nov	52.1	54.1	48.7	52.6
Dec	47.4	45	44.3	51.3

TABLE 9: COMPARISON OF MONTHLY β_0 VALUES (%) AT 4 SITES USING 1-(b) APPROACH WITH ITU MAPS

Months	ITU Values	AUH	DXB	SHJ	RAK
February	30	55.9	58.3	55.32	62.4
May	75	69.1	71.9	60.6	63.2
August	70	57.5	71.1	62.9	64.2
November	40	52.1	54.2	48.9	52.7

F. $\Delta N_{0.065}$ at 65 m Layer and Analysis of Point Refractivity Gradient ($dN_{1\%}$)

The $\Delta N_{0.065}$ values calculated using approaches 1-(a) and 1-(b) for different time percentages at AUH are compared with ITU maps in Table 10. Bilinear interpolation has been used to get exact values of $\Delta N_{0.065}$ at AUH from the corresponding ITU data files for the given coordinates at different time percentages. The results are not in good concurrence with ITU values. Considering the absolute values of $\Delta N_{0.065}$ results, the ITU values are found to be overestimated for 10% of time, while they are under-estimated for 90% and 99%. For 1% of time, the estimated ITU value is below the calculated value using the reference 1-(b) approach. The cumulative distributions of $\Delta N_{0.065}$ using the 1-(b) approach at the sites with similar surface refractivity profiles are provided in Fig. 22. Table 11 provides $\Delta N_{0.065}$ values obtained at AUH, DXB, SHJ and RAK sites at different time percentages. The highest absolute $\Delta N_{0.065}$ values for 1% and 10% are shown in AUH and DXB, respectively, while RAK shows the top values for larger time percentages.

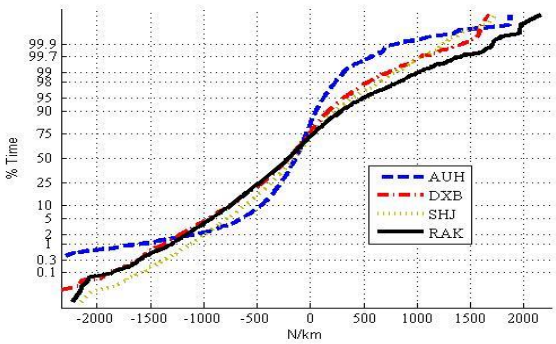

Fig. 22. Comparison of cumulative distributions of ΔN0.065 at 4 sites using 1-(b) approach (1997-2013)

TABLE 10: COMPARISON OF $\Delta N_{0.065}$ VALUES (N/km) AT AUH USING 1-(a) AND 1-(b) APPROACHES WITH ITU MAPS

Time %	ITU values	1-(a)	1-(b)
1%	-952.42	-722.5	-1604.5
10%	-553	-344.9	-460.9
50%	-92.824	-89.8	-142
90%	-4.38	76.8	51.3
99%	38.86	305.4	307.6

TABLE 11: VALUES OF $\Delta N_{0.065}$ NOT EXCEEDED FOR DIFFERENT TIME PERCENTAGES AT 4 SITES

Time %	AUH	DXB	SHJ	RAK
1%	-1604.5	-1378.8	-1122.3	-1300.1
10%	-460.9	-760.3	-616.3	-752.8
50%	-142	-198.6	-152.3	-202.7
90%	51.3	173.7	232.8	291.3
99%	307.6	733.6	803.7	1025.1

III. CONCLUSIONS

Seventeen years of local surface and radiosonde meteorological data were used to study the vertical refractivity profile for three critical atmospheric layers within the first kilometer above the ground surface.

The surface meteorological measurements using the radiosonde were found to be slightly different from the measurements obtained from fixed weather stations which are usually more accurate due to higher stability.

A new approach was proposed for utilizing the upper-air refractivity from a radiosonde site in the surrounding sites with similar surface conditions. The analysis of surface refractivity was used for the evaluation of vertical refractivity profile in areas where radiosonde data are not available. For ΔN analysis at 1 km, the same approach was used for the sites where surface profiles were not so consistent with those from the radiosonde location assuming that the atmosphere gets increasingly horizontally homogeneous at higher altitudes. Exponential prediction models were also used for the ΔN prediction at all sites. The analysis of the given approaches for evaluating the mean vertical refractivity profiles showed that higher concurrency with radiosonde measurement could be obtained using the new proposed approach in this study. However, the range of variation was found to be higher for altitudes of 100 m and below. Some differences were observed in monthly refractivity gradient profiles at certain sites with similar mean surface profiles, in particular for low altitudes below 100 m. This could be attributed to the fact that the measurements at a given time were not necessarily the same at these sites over the whole period, and that any small change in Ns value results in large disagreement in ΔN due to the low decimal number in the denominator of the linear ΔN equation for low heights.

A new approach was used to evaluate *k*-factor from the weighted average ΔN at three layers, which is recommended to be applied in other areas. The mean *k* value of -11.7 indicated the prevalence of the ducting phenomenon in one area under study.

The results obtained in this study can be useful for areas with a subtropical climate, where weather is hot and humid

Author draft, IEEE Trans on Antennas and Propagation, VOL. 63, NO. 9, SEPTEMBER 2015, pp. 4057 - 4068, DOI: 10.1109/TAP.2015.2452937

over the year. The proposed approaches can also be applied in other areas with different climates. The vertical refractivity gradients in areas where upper air measurements are not available can be evaluated from the analysis of surface refractivity profiles. The upper air data are measured at a single Radiosonde site and used in surrounding areas with similar surface profiles. In addition, the new weighted average approach at various atmospheric layers can be applied to estimate effective earth radius factor.

The β_0 analysis at four sites indicated that the probability of anomalous propagation exceeded 44% for all months and reached up to 71% at certain locations within the summer.

The results obtained in this study for the Gulf region would also suggest the necessity to revise the ITU maps, in particular for similar subtropical climate, based on recently gathered long-term local meteorological data from more radiosonde sites worldwide, since ITU values are being widely used for the design of wireless communication systems.

Based on the results presented in this work, it is recommended to apply similar approach to evaluate the vertical refractivity profiles in the areas surrounding a radiosonde location and for areas with similar surface refractivity conditions.

ACKNOWLEDGMENT

The authors would like to express their gratitude to the National Center of Meteorology in the United Arab Emirates for providing the raw meteorological data used in this work and the Radio Frequency and Computational Electromagnetics Research Group of Bradford University in providing the software requirements.

REFERENCES

[1] M. I. Skolnik, *Introduction to Radar Systems*, 3rd ed.: McGraw-Hill Inc., 2001.

[2] I.-R. R. P.453-10, "The radio refractive index: its formula and refractivity data," *International Telecommunication Union, ITU,* 2012.

[3] I.-R. R. PN.310-9, "Definitions of terms relating to propagation in non-ionized media," *International Telecommunication Union, ITU,* 1994.

[4] R. L. Freeman, *Radio System Design for Telecommunications*: John Wiley, 1997.

[5] I. R. Bureau, "Handbook on Radiometeorology," *International Telecommunication Union,* Geneva, 1996.

[6] T. G. Hayton and K. H. Craig, "Use of Radiosonde Data in Propagation Prediction," presented at the IEE, Savoy Place, London WC2R OBL, UK, 1996.

[7] L. S., "Investigation of surface refractivity and refractive gradients in the lower atmosphere of Norway," presented at the COST 235, CP 121, March 1993.

[8] A. K. P. Marsh, T. G. Hayton, and K. H. Craig, "Initial Comparison of Refractivity Parameters Derived from Radiosondes and Psychrometers in France," in *COST255, CP42010*, Oct. 1997.

[9] B. L. and S. H., "Refractivity Over France: First Results of ARGOS Experiment," *COST255, CP32003,* May 1997.

[10] K. H. Craig and T. G. Hayton, "Investigation of β0 values derived from ten years radiosonde data at 26 stations," presented at the COST 235, CP 182, Oct. 1993.

[11] K. H. Craig and T. G. Hayton, "Refractivity parameters from radiosonde data," in *AGARD Conference On Propagation Assessment in Coastal Environments*, Germany, 1994, pp. 1-12.

[12] A. AbouAlmal, R. A. Abd-Alhameed, K. Al-Ansari, H. AlAhmad, C. H. See, and S. M. Jones, "Statistical Analysis of Refractivity Gradient And β0 Parameter In The Gulf Region," The paper is currently under publication in the IEEE Transaction On Antennas and Propagation.

[13] Abdulhadi Abu Al-mal and K. Al-Ansari, "Calculation of Effective Earth Radius and Point Refractivity Gradient in UAE," *International Journal of Antennas and Propagation,* vol. 2010, 2010.

[14] Kifah Al-Ansari, Abdulhadi AbuAl-Mal, and R. A. Kamel, "Statistical Analysis of Refractivity in UAE," *Internationl Symposium on Rainfall Rate and Radiowave Propagation, India, Published by American Institute of Physics Conference Proceedings,* vol. 923, pp. 232-247, 2007.

[15] K. Al Ansari and R. A. Kamel, "Correlation Between Ground Refractivity and Refractivity Gradient and Their Statistical and Worst Month Distributions in Abu Dhabi," *Antennas and Wireless Propagation Letters, IEEE,* vol. 7, pp. 233-235, 2008.

[16] A. AbouAlmal, R. A. Abd-Alhameed, A. S. Hussaini, T. Ghazaany, Z. Sharon, S. M. R. Jones, and J. Rodriguez, "Comparison of Three Vertical Refractivity Profiles In The Gulf Region," in *Wireless Conference (EW), Proceedings of the 2013 19th European*, 2013, pp. 1-4.

[17] A. AbouAlmal, R. A. Abd-Alhameed, S. M. R. Jones, and H. Al-Ahmad, "New Approaches and Algorithms for the Analysis of Vertical Refractivity Profile below 1 km in a Subtropical Region," Under Review and Publication in IEEE Transactions on Antennas and Propagation.

[18] S. S. MENTES and Z. KAYMAZ, "Investigation of Surface Duct Conditions over Istanbul, Turkey," *Journal of Applied Meteorology And Climatology,* vol. 46, 2006.

[19] Dominguez M. A., Benarroch A., and Riera J. M., "Refractivity Statistics in Spain: First Results," in *COST 255, CP52004*, May 1998.

[20] O. Jicha, P. Pechac, V. Kvicera, and M. Grabner, "Estimation of the Radio Refractivity Gradient From Diffraction Loss Measurements," *Geoscience and Remote Sensing, IEEE Transactions on,* vol. 51, pp. 12-18, 2013.

[21] O. Jicha, P. Pechac, V. Kvicera, and M. Grabner, "Estimation of radio refractivity profile gradient from multiple LOS links using artificial neural networks — First results," in *Antennas and Propagation (EUCAP), 2012 6th European Conference on*, 2012, pp. 1174-1177.

[22] I.-R. R. P.452-12, "Prediction Procedure for the Evaluation of Microwave Interference between stations on the surface of the earth at the frequencies above about 0.7 GHz," *International Telecommunication Union, ITU,* 2005.

[23] "ITU-R Recommendation P.530-14: Propagation data and prediction methods required for the design of terrestrial line-of-sight systems," *International Telecommunication Union,* 2012.

[24] A. AbouAlmal, R. A. Abd-Alhameed, K. Al-Ansari, H. Al-Ahmad, C. H. See, S. M. R. Jones, and J. M. Noras, "Statistical Analysis of Refractivity Gradient And β0 Parameter In The Gulf Region," *Antennas and Propagation, IEEE Transactions on,* vol. 61, pp. 6250-6254, 2013.

[25] A. T. Adediji, M. O. Ajewole, and S. E. Falodun, "Distribution of radio refractivity gradient and effective earth radius factor (k-factor) over Akure, South Western Nigeria Original Research Article," *Journal of Atmospheric and Solar-Terrestrial Physics,* vol. 73, pp. 2300-2304, Oct. 2011.

Abdulhadi AbouAlmal received his Bachelor degree in communication engineering from Ajman University of Science and Technologies (AUST), in 2007, and the Master of Science in engineering systems? management from the American University of Sharjah (AUS) in 2011. He is currently completing his PhD degree in wireless communication at the University of Bradford, UK. After obtaining his undergraduate degree, he joined the research unit of Sharjah University and the school of Engineering in AUS and AUST universities, as a research and teaching assistant for around two years. Since 2008, he has been with the leading telecom operator in the Middle East (Emirates Telecommunication Corporation, Etisalat) as a manager of wireless networks planning. He used to be the coordinator of Etisalat, UAE and Arab spectrum management group in the world conferences and Study Group 3 meetings of the International Telecommunication Union (ITU). His research interests are in wireless networks deployment optimization, microwave fading and wave propagation

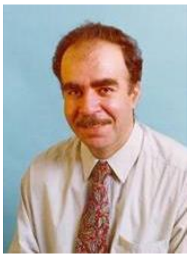

Raed A. Abd-Alhameed is Professor of Radio Frequency, antennas and computational Electromagnetic techniques at the University of Bradford. He has over 20 years research experience and has published over 400 academic journal and conference papers; in addition he is co-authors of three books and several book chapters. He is Principal Investigator for the EPSRC-funded project 'Multi-Band Balanced Antennas with Enhanced Stability and Performance for Mobile Handsets'. He has also been a named co-investigator in several funded research projects including: 1) Nonlinear and demodulation mechanisms in biological tissue (Dept. of Health, Mobile Telecommunications & Health Research Programme and 2) Assessment of the Potential Direct Effects of Cellular Phones on the Nervous System (EU: collaboration with 6 other major research organisations across Europe). He is the leader for several successful knowledge Transfer Programmes such as with Pace plc, YW plc, Seven Technologies Group ltd, Emkay ltd, Two World ltd and IETG ltd. He was awarded the business Innovation award for his successful KTP with Pace on the design and implementation of MIMO antenna systems; and recently Excellence in KTP project with Seven Technologies Group ltd. He is the chair of several successful workshops on Energy Efficient and Reconfigurable Transceivers (EERT): Approach towards Energy Conservation and CO_2 Reduction that addresses the biggest challenges for the future wireless systems. He is also invited as keynote speaker for several International conferences such as, ICST, ITA and EPC; in addition to chair many research sessions. He has also appointed as guest editor for the IET Science, Measurements and Technology Journal since 2009. He is also a research visitor for Wrexham University, Wales since Sept 2009 covering the wireless and communications research areas. His current research interests include hybrid electromagnetic computational techniques, EMC, antenna design, low SAR antennas for mobile handset, bioelectromagnetics, RF mixers, active antennas, beam steering antennas, MIMO antennas, Energy efficient PAs, RF predistorter design including biological cell modelling for breast cancer applications. Prof Abd-Alhameed is the Fellow of the Institution of Engineering and Technology, Fellow of Higher Education Academy and a Chartered Engineer.

Steve Jones is a Senior Lecturer in Telecommunications and Head of Electrical Engineering in the School of Electrical Engineering and Computer Science, Faculty of Engineering and Informatics at the University of Bradford. Since joining the University in 1987, he has worked on a wide variety of projects in the area of satellite slant-path propagation (e.g. 10 GHz bistatic-scatter, 11/14 GHz scintillation and ice depolarization with Olympus) and mobile radio propagation (notably Copernicus, Mobile VCE and TEAMS projects). He served as an Associate Editor for the IEEE Transactions on Antennas and Propagation 2004-8. Recently, he has worked on multiple-antenna technologies, signal processing and propagation modelling for broadband wireless access systems.

Hussain Al-Ahmad (S'78-M'83-SM'90) received his Ph.D in Signal Processing from the University of Leeds, UK in 1984. He worked at Portsmouth University, UK, Leeds Beckett University, UK, Kuwaiti Faculty of Technological Studies, University of Bradford, UK and Etisalat University College, UAE. Currently he is a full professor at the Department of Electrical and Computer Engineering, Khalifa University of Science, Technology and Research, UAE. His primary research interests are in signal and image processing. Prof. Al-Ahmad is a fellow of the IET, Chartered Engineer, member of BCS, Chartered IT Professional and a fellow of the Royal Photographic Society. He is the vice chair of the IEEE UAE section and Chair of the IEEE UAE Education Chapter. He was the secretary of the IEEE Kuwaiti section, the chair of the IEEE UAE computer chapter and vice chair of the IEEE UAE signal processing and communication chapter. He is the author and co-author of 115 journal and conference papers. He has supervised successfully 30 PhD and Master students in the UK and UAE. He has delivered short courses and seminars in Europe, Middle East and Korea. He was member of the technical program committees of many IEEE conferences such as EDUCON, ICECS, ICSPC, ISSPIT and ICIP.